Proximal Bacterial Lysis and Detection in Nanoliter Wells Using Electrochemistry

Justin D. Besant,[†] Jagotamoy Das,[‡] Edward H. Sargent,[§] and Shana O. Kelley[†,‡,⊥,*]

[†]Institute for Biomaterials and Biomedical Engineering, [‡]Department of Pharmaceutical Sciences, Leslie Dan Faculty of Pharmacy, [§]Department of Electrical and Computer Engineering, Faculty of Applied Science and Engineering, and [⊥]Department of Biochemistry, Faculty of Medicine, University of Toronto, Toronto, ON, Canada M5S 3M2

ABSTRACT Rapid and direct genetic analysis of low numbers of bacteria using chip-based sensors is limited by the slow diffusion of mRNA molecules. Long incubation times are required in dilute solutions in order to collect a sufficient number of molecules at the sensor surface to generate a detectable signal. To overcome this barrier here we present an integrated device that leverages electrochemistry-driven lysis less than 50 μm away from electrochemical nucleic acid sensors to overcome this barrier. Released intracellular mRNA can diffuse the short distance to the sensors within minutes, enabling rapid and sensitive detection. We validate this strategy through direct lysis and detection of *E. coli* mRNA at concentrations as low as 0.4 CFU/μL in 2 min, a clinically relevant combination of speed and sensitivity for a sample-to-answer molecular analysis approach.

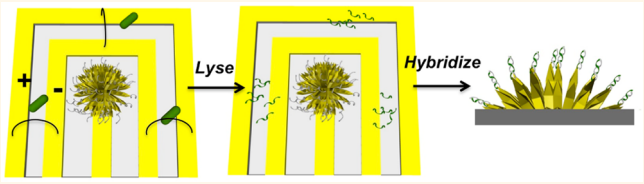

KEYWORDS: bacterial detection · cell lysis · electrochemical detection · microelectrodes

New strategies for rapidly detecting low levels of bacteria are urgently needed to control and manage infectious disease.[1] No existing method simultaneously satisfies the needed speed and sensitivity requirements to detect sufficiently low levels of bacteria in a clinically-relevant time period.[2] Culture, the gold standard for diagnosis for most types of bacterial infection diagnosis, requires hours to days to amplify the bacteria to visibly detectable levels. Enzymatic amplification methods such as the polymerase chain reaction (PCR) are complex to automate and often require sample purification that slows analysis.[3,4]

A wide variety of molecular sensors have been developed to address the limitations of culture and PCR.[5−8] The direct detection of nucleic acid sequences using chip-based sensors has been pursued for some time as an attractive solution.[9−14] The use of mRNA sequences such as that corresponding to the RNA polymerase β (rpoβ) subunit can provide species-level identification of bacteria,[15] and many copies of mRNA may exist in a single cell which provides an inherent signal enhancement. However, using this type of biomarker to rapidly detect bacteria at clinically relevant levels remains a challenge; the long diffusion times of large mRNA molecules impose an inherent trade-off between speed and sensitivity of detection.[16,17] In a typical sample-to-answer detection scheme, bacteria are lysed in a lysis chamber and the homogeneous lysate is then transported to a detection chamber (Figure 1A).[18] As each bacterium may harbor multiple copies of the target mRNA, prior to lysis, the molecules are present at a locally high concentration inside each bacterium. However, after lysis, intracellular mRNA is released into bulk solution, and thus the overall concentration of mRNA is very low. When sensing low concentrations of mRNA, long incubations times are required in order to accumulate enough target molecules at the sensor surface to generate a detectable signal.

Here, we propose a novel approach to rapid genetic analysis that uses an electrochemical approach to lyse bacteria in close proximity to a microelectrode where their mRNA can be analyzed. Proximal electrochemical lysis shortens the required distance over which the target mRNA molecules must diffuse. This approach provides a 10-fold improvement in performance and permits rapid analysis of bacteria at clinically relevant levels.

* Address correspondence to shana.kelley@utoronto.ca.

Received for review July 10, 2013 and accepted August 9, 2013.

Published online August 09, 2013
10.1021/nn4035298

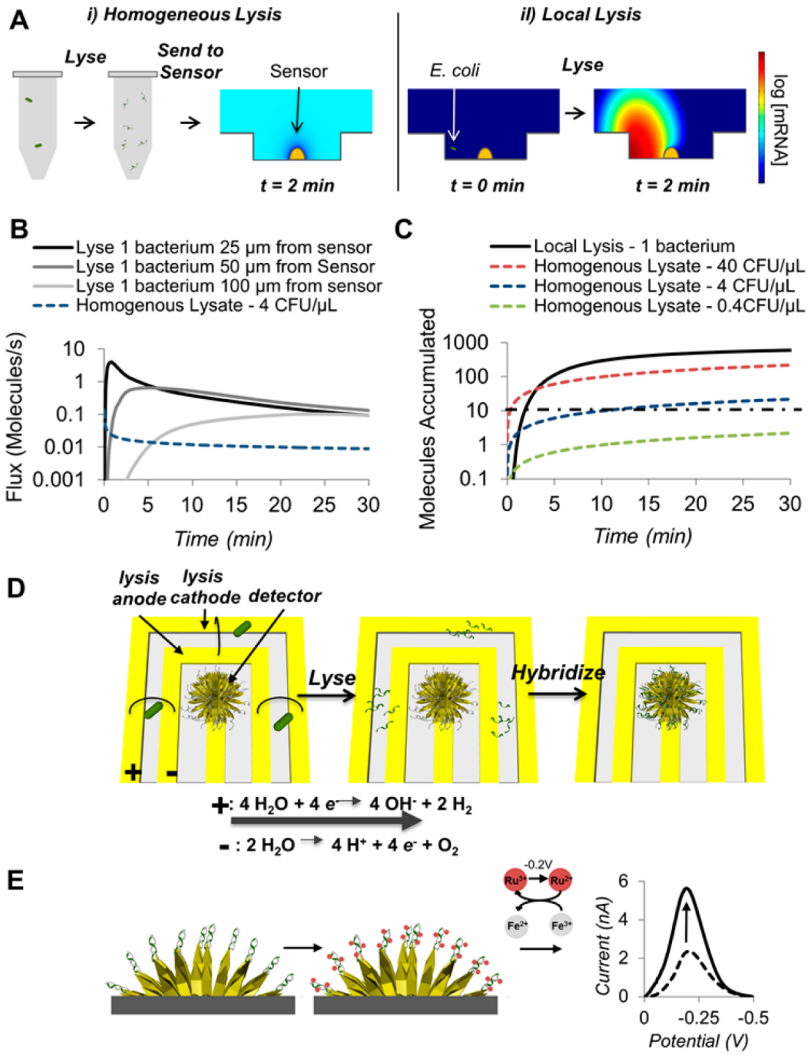

Figure 1. Schematic of lysis and electrochemical readout. (A) (i) Typically, bacteria are lysed in bulk solution, and the homogeneous lysate is transferred to the sensor. (ii) In an alternative proximal lysis approach, bacteria are lysed in the vicinity of the sensor, and released mRNA can rapidly diffuse the short distance to the sensor. (B) Diffusional flux of mRNA released from a single bacterium harboring 1400 transcripts. The flux from lysis at varying distances from the sensor is compared to the flux from homogeneous lysate from 4 CFU/μL. (C) Molecules accumulated at the sensor over time after local lysis (50 μm away) of a single bacterium compared to homogeneous lysate at varying concentrations. Detecting less than $\sim$1 CFU/μL in 5 min is not possible in a homogeneous lysate. In contrast, intracellular RNA from just a single bacterium lysed locally accumulates within minutes at the sensor surface. The dashed black line represents a typical threshold for detection of 10 molecules. (D) Each well contains two lysis electrodes and an NME sensor. Bacteria are lysed electrochemically by an applied potential. Released intracellular mRNA rapidly hybridizes to the complementary PNA probe molecules functionalized on the NME surface. (E) The amount of hybridized mRNA is read using an electrocatalytic reporter pair and DPV to measure the peak current before and after hybridization.

RESULTS AND DISCUSSION

Summary of Approach. Detection of mRNA using chip-based sensors is limited by the rate of molecular diffusion to the sensor. Molecules of bacterial mRNA, which can be up to thousands of base pairs long, have low diffusion coefficients compared to short synthetic oligomers, and long time scales are therefore required to collect enough molecules to generate a robust response.[19] To study the diffusional flux of analytes at the sensor after lysis, we created a model of a single *E. coli* inside a well that contains a 20 μm hemispherical sensor. We assumed each *E. coli* contained multiple copies of RNA polymerase β subunit (rpoβ), a 4000 bp transcript. We assumed a copy number of 1400 as calculated previously.[17] Figure 1B compares the diffusional flux of the analytes at the sensor as a function of time for the homogeneous and local lysis approaches. In the homogeneous lysis case, the flux is low and nearly constant. In the local lysis approach, the flux rapidly increases in the first minutes as the analytes reach the sensor and slowly decays as the molecules diffuse away. Figure 1C shows the number of analyte molecules captured at the sensor surface over time for both lysis scenarios. Rapidly (<30 min) detecting less than 1 CFU/μL is not possible with a homogeneous lysis approach as no analyte molecules are captured

after 30 min. On the other hand, if just a single bacterium is lysed 50 μm from the sensor, many target analytes will accumulate on the sensor surface within minutes.

In light of the findings from our diffusional model, we designed a device that would minimize the distance between the site of cell lysis and mRNA detection. The device featured electrodes for electrochemical lysis that surrounded a detection sensor (Figure 1D). Previous studies have shown that hydroxide ions can be produced locally to initiate cellular lysis, but this approach has primarily been used in bulk solution as a means to prepare samples for analysis using PCR or other detection approaches.[20−22] Here, lysis electrodes were placed within 50 μm of a microelectrode sensor, which allows large mRNA molecules to diffuse to the sensor within 10 min. The reaction that initiates cell lysis is based on the production of hydroxide ions from water at a cathode at a potential of 20 V. Hydroxide ions can break down bacterial membranes, causing the contents of the bacteria, including the nucleic acids, to be released into solution.

The placement of a chip-based sensor in close proximity to the lysis electrodes provides the potential for very sensitive analysis of bacterial cells because limited diffusion is required of the molecules that provide information on cellular identity. The functionalization of a nearby sensor with a thiolated probe molecule that is complementary to a unique portion of a bacterial mRNA allows capture of the marker if bacteria are present within a sample undergoing analysis. The presence of bound target mRNA can be read using an electrochemical reporter system that senses the change in electrostatics at the sensor surface (Figure 1E).[23] $Ru(NH_3)_6^{3+}$ ions accumulate at the sensor surface and serve as electron acceptors. $Fe(CN)_6^{3-}$ ions serve to reoxidize Ru(II) as it is made electrochemically and regenerate the electron acceptor to make the reaction electrocatalytic. Differential pulse voltammetry provides an effective sampling method that can be used to investigate whether current levels rise above a threshold that indicates that a sample is positive for a particular pathogen.

Design and Validation of Lysis Electrodes for Electrochemical Hydroxide Generation. Given that large applied potentials could disrupt the bond between a probe sequence and the sensor, thereby compromising the integrity of the surface assembled monolayer, we simulated the electric fields generated by different lysis electrode geometries (Figure 2A,B). Lysis electrodes which sandwich the sensor induce a high potential at the sensing electrode which could reduce probe coverage by dissociating the gold−thiol bond (Figure 2A). Figure 2B shows an alternative layout in which both lysis electrodes wrap around the sensing electrode. The electrodes act as an on-chip faraday cage to shield the sensor from the electric fields. We chose this layout to minimize the electric fields experienced by the sensor.

Another feature of the device we fabricated is patterned wells that contain the lysis and sensing electrodes to enable the contents of the bacterial cells to remain close to the sensor. The wells introduced on the surface of the chip hold 1 nL of liquid and were generated using SU-8 and patterned using photolithography. Nanostructured microelectrode (NME) sensors were plated within the wells and were shown to

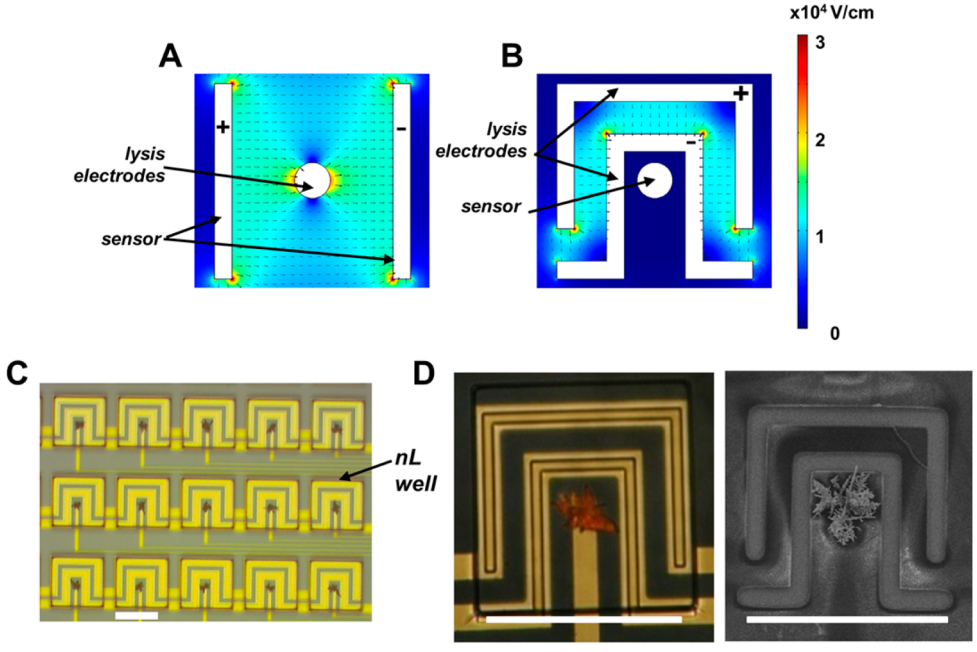

Figure 2. Device design. Simulations of the electric fields induced by lysis electrodes which span the sensor (A) and wrap around the sensor (B). (C) Optical microscopy image of NMEs electrodeposited into the well array. (D) Optical microscopy and scanning electron microscopy images of an electrodeposited NME. Scale bars represent 100 μm.

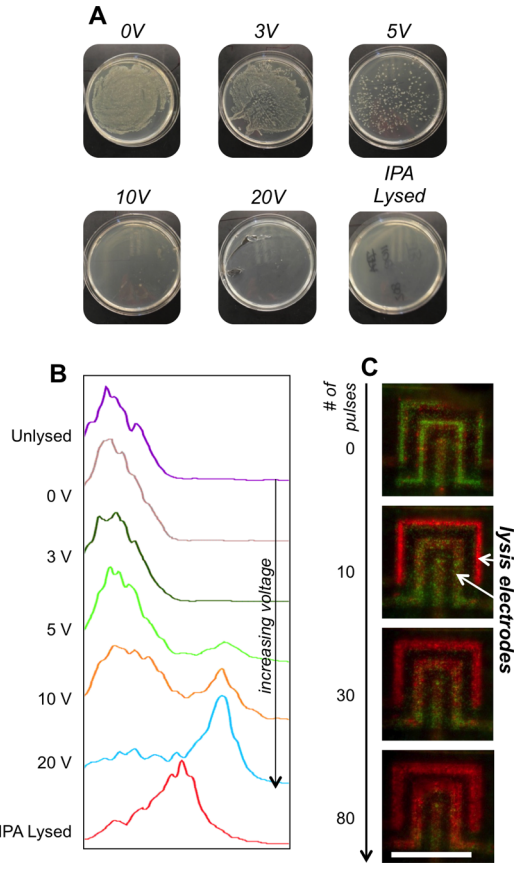

Figure 3. Validation of electrochemical lysis. (A) Effect of applied potentials on E. coli viability after incubating on agar plates. IPA was used as a positive control. (B) Uptake of PI measured by flow cytometry as a function of voltage. IPA is used as a positive control. (C) Uptake of PI measured with optical microscopy as a function of the number of pulses applied. E. coli expressing GFP are green, and E. coli that uptake PI are red. Scale bars represent 100 μm.

exhibit similar morphologies to what has been demonstrated previously (Figure 2C,D).[17,18,24]

As an initial assessment of lysis, we measured *E. coli* growth on agar plates after they were subjected to on-chip electrochemical lysis (Figure 3A). We applied pulse voltages from 0 to 20 V at 1 Hz for 1 min to *E. coli* and allowed the lysate to incubate on agar plates overnight. *E. coli* viability dropped after applying 5 V, and no growth was observed after applying 20 V. While this approach is an indirect measure of whether lysis is occurring, it provides a means to identify an interesting potential range to look for membrane permeability.

To study whether lysis made the *E. coli* membrane permeable, we measured cellular uptake of propidium iodide (PI), a fluorescent dye which intercalates with DNA (Figure 3B). Cellular uptake of PI is used as an indicator of lysis as PI cannot cross intact cell membranes. Using flow cytometry, we measured propidium iodide uptake as a function of pulse voltage. Increasing voltage caused greater uptake of propidium iodide, with the largest uptake at 20 V.

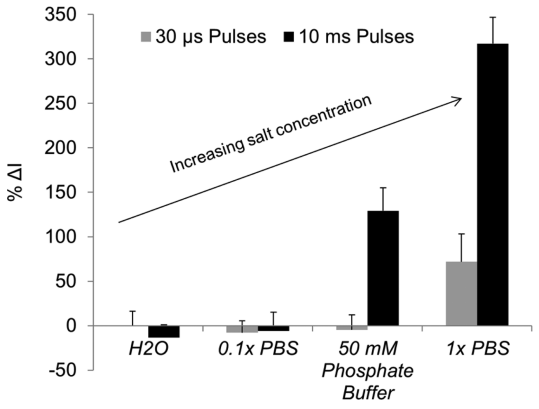

Figure 4. Effect of lysis on probe integrity. Percent change in magnitude of peak oxidation currents of $Fe(CN)_6^{4-}$ measured before and after on-chip lysis. The percent increase in current measured after applying 30 μs and 10 ms pulses in various buffers. High percentage changes indicate that the probe is removed from the surface. Error bars represent standard error.

Using fluorescent microscopy, we visualized PI uptake in real time (Figure 3C). Voltage pulses (20 V) were applied to *E. coli* expressing green fluorescent protein (GFP) in the presence of PI. We observed greater PI uptake as increasing number of voltage pulses were applied. *E. coli* lyse first at the positive outer electrode and then near the grounded inner electrode.

Identification of Compatible Solution Conditions for Electrochemical Lysis and Detection. Initiating lysis close to a chip-based sensor has the potential to improve detection limits but may also introduce issues that would interfere with the function of the sensors. As discussed above, the presence of a strong field could interfere with the attachment of the probe to the sensor. In addition, the ions generated electrochemically could degrade the probe molecules.[25]

We tested different lysis conditions and investigated whether probe molecules were dissociating from the sensor surface. An assay based on the blocking of the surface in the presence of probe was used, where signals generated by $Fe(CN)_6^{4-}$ were analyzed. The iron reporter group is repelled by the anionic probe, and if stripping occurred, the signal it generates would increase.

As shown in Figure 4, differing levels of probe stripping were observed when buffer conditions were varied. Lysis performed in water with short (30 μs) or long (10 ms) pulses did not cause probe dissociation. However, lysis in 1× phosphate-buffered saline did cause damage with large signal changes occurring for both pulse times. Diluting the PBS or the use of phosphate buffer attenuated this effect. In PBS, the presence of chloride ions likely contributes to the production of hypochlorite ions after the production of Cl_2 at the anode. Hypochlorite is highly reactive and persists in buffered solutions and is expected to cause significant damage both to immobilized probes and the molecules being liberated within a sample. It is therefore desirable to avoid generating this species.

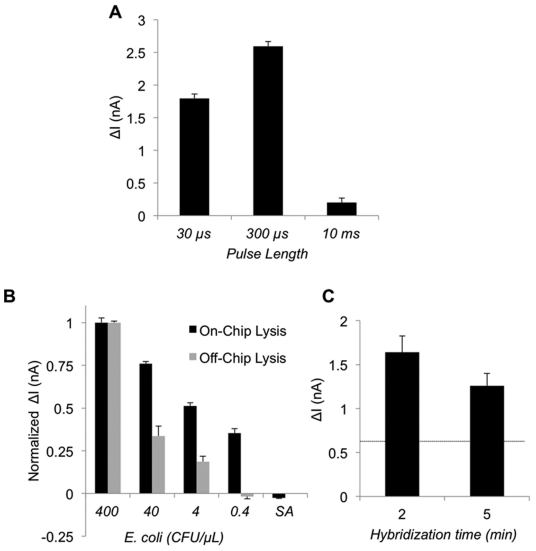

Figure 5. Lysis and electrochemical detection of E. coli. (A) Effect of electrical lysis pulse length on the electrochemical signal change. (B) Concentration-dependent signal change of E. coli lysed on-chip as compared to E. coli lysed off-chip. The data were normalized to the signal from 400 CFU/μL. (C) Hybridization time dependence of the signal from E. coli lysed on-chip. The dashed line corresponds to the average signal change in the absence of E. coli. Error bars represent standard error.

Lysis in phosphate buffer, especially with short pulses, resulted in minimal probe loss and provides buffering capacity to ensure that samples only transiently experience elevated hydroxide levels and provides ionic strength to promote hybridization on the sensor surface. This buffer system was therefore identified as the best set of solution conditions that was compatible with both electrochemical lysis and detection.

Bacterial Detection with Proximal Lysis. With effective lysis demonstrated, the detection of bacteria using the devices was tested. A series of studies were conducted that focused on the effect of lysis pulse length on detection of *E. coli* (Figure 5A). Increasing the pulse time from 30 to 300 μs increased the amount of current change generated with a solution of 400 CFU/μL *E. coli* cells per microliter, indicating greater lysis efficiency with the longer pulses. The optimal current at 300 μs is likely due to the competing effects of hydroxide generation. High hydroxide concentrations lead to efficient lysis but also to degradation of the target molecules. Below 300 μs, the lysis is not as efficient, while above 300 μs, the target likely degrades due to excessive hydroxide concentration and the probe is removed from the sensor which causes a lower current change.

To evaluate the detection limit of the sensors with proximal lysis, *E. coli* were serially diluted from 400 to 0.4 CFU/μL (Figure 5B). *E. coli* were lysed on-chip by applying the optimal 300 μs pulses for 1 min, and the lysate was allowed to incubate at 37 °C for 30 min. The 5000 CFU/μL *S. aureus* was used as a negative control. *E. coli* were detected with a limit of detection of 0.4 CFU/μL and high specificity as no signal was observed from *S. aureus*.

The sensitivity enhancement provided by the combination lysis/detection device was tested by challenging the sensors with serial dilutions of *E. coli* lysed off-chip. The limit of detection of the device when challenged with *E. coli* lysate prepared off-chip was only 4 CFU/μL, which is 10 times higher than when *E. coli* were lysed on-chip. This indicates that lysis in close proximity to the sensors provided a 10-fold sensitivity advantage.

In addition to providing enhanced detection limits, proximal lysis should also speed the progress of hybridization and produce fast results. To determine the time dependence of the detection approach, we challenged the sensor with *E. coli* at 0.4 CFU/μL using 2 and 5 min hybridization times (Figure 5C). We observed a positive signal from 0.4 CFU/μL after both 2 and 5 min hybridization periods, indicating that the sensor has a rapid response time. This is a record-breaking level of speed and sensitivity combined in a single sensor system. The previous sensitivity record for direct electrochemical detection of mRNA in crude lysate is 1 CFU/μL after a 20 min incubation time.[18] Here we show detection of 0.4 CFU/μL within 2 min.

Real sample matrices have a wide range of pH and salt concentrations which need to be controlled in proximal electrochemical lysis. To use this device with complex matrices, the sample could be prediluted in the appropriate buffer. Alternatively, this device could be coupled to a preconcentration step to separate the bacteria of interest from the sample and allow for buffer exchange.

CONCLUSIONS

We developed an integrated device capable of electrochemical lysis and detection of *E. coli* at concentrations as low as 0.4 CFU/μL in 2 min. Lysing in the vicinity of the sensors allowed high concentrations of released intracellular mRNA to reach the sensor rapidly. Our experiments highlight the importance of optimizing the buffer and electrode geometry when lysing nearby surface-modified electrodes in order to maintain the integrity of the probe monolayer and provide a powerful sample-to-answer approach for bacterial detection.

METHODS

Simulations. Simulations of electric fields for various lysis electrode designs were conducted using COMSOL Multiphysics. The applied voltages were set to keep the average field constant across both geometries.

Simulations of the flux of analyte molecules at the sensor surface were calculated using a COMSOL model.

These calculations are described in the Supporting Information.

Device Fabrication. Devices were fabricated by the Canadian Photonics Fabrication Centre (Ottawa, ON) on 300 μm thick 6 in. silicon wafers coated with 450 nm of thermally grown SiO_2. To pattern the electrodes, 300 nm Au was deposited on a 25 nm Ti adhesion layer. After patterning the electrodes using standard photolithography and wet etching, the electrodes were passivated with 500 nm SiO_2 using plasma-enhanced chemical vapor deposition. The lysis electrodes, contacts, and apertures were exposed using reactive ion etching. Wells were patterned using SU-8 30-25 (Microchem, Newton, MA) using photolithography. The devices were diced and fixed to the bottom of a custom-designed PMMA reservoir (QuickCUTCNC, Atlanta, GA).

NME Electrodeposition. Nanostructured microelectrodes (NMEs) were electrodeposited using a two-step process using a three-electrode setup with a Pt counter electrode and a Ag/AgCl reference electrode. To grow a sensor with a large footprint, we applied 0 mV with respect to the Ag/AgCl reference electrode for 20 s in a solution of 50 mM $HAuCl_4$ and 0.5 M HCl. Sensors were decorated with nanostructured features by applying −250 mV in a solution of 5 mM $PdCl_2$ and 0.5 M $HClO_4$ for 5 s.

Preparation of Bacterial Samples. *E. coli* (Invitrogen, Carslbad, CA) and *S. aureus* (ATCC) were cultured in an incubating shaker at 33 °C in LB Miller and tryptic soy agar broth, respectively. Concentrations were measured using optical density measurements at 600 nm with a UV−vis spectrometer (Agilent, Santa Clara, CA) and by counting the number of colonies on agar plates incubated overnight at 37 °C. Using centrifugation, the growth medium was replaced with the appropriate buffer before lysis. To assess cell viability, 100 μL of lysate was spread on LB agar plates and incubated overnight at 37 °C. *E. coli* were lysed off-chip using OmniLyse (Claremont Bio, Upland, CA).

Flow Cytometry. *E. coli* were diluted to 1×10^7 CFU/mL in various buffers. Potentials from 0 to 20 V were applied to lysis electrodes using a 1 Hz repetition rate for 60 s. After lysis, samples were incubated with 2 μg/mL propidium iodide for 30 min in the dark. Measurements were made using a BD FACS Canto flow cytometer and plotted as histograms of fluorescence intensity.

Fluorescent Microscopy. *E. coli* expressing GFP were diluted to 1×10^7 CFU/mL in the appropriate buffer and lysed with varying numbers of 20 V pulses (30 μs pulse time). Samples were incubated with 2 μg/mL propidium iodide, and red and green fluorescent images were acquired with a Nikon Eclipse LV150 microscope.

Synthesis and Purification of PNA Probes. Probes complementary to *E. coli* rpoβ mRNA (4029 bp) were designed with the following sequence: NH_2-Cys-Gly-Asp-ATC TGC TCT GTG GTG TAG TT-Asp-$CONH_2$. Probes were synthesized using a protein Technologies Prelude peptide synthesizer and purified using reverse-phase high-performance liquid chromatography. Probe concentration was calculated using the extinction coefficient and the absorbance at 260 nm.

Sensor Functionalization, Lysis, And Hybridization. Sensors were functionalized with 1 μM PNA probe and 9 μM mercaptohexanol for 30 min at room temperature. Chips were washed twice for 5 min with 1× PBS buffer after probe deposition. *E. coli* and *S. aureus* were diluted to the appropriate concentration in 50 mM phosphate buffer, and 50 μL was added to the chip. After washing, potentials were applied to lysis electrodes using 1 Hz pulses with varying voltages and pulse times. The chip was incubated in a humidity chamber for 2 to 30 min at 37 °C followed by washing twice with PBS for 5 min. After washing, DPV measurements were performed following probe deposition and sample hybridization in the electrocatalytic solution.

Electrochemical Masurements. For all electrochemical measurements, we used a three-electrode setup with a Ag/AgCl reference electrode and Pt counter electrode connected to a potentiostat (BASi, West Lafayette, IN). To measure the effect of lysis on probe detachment, NMEs modified with a PNA probe were scanned from 0 to 0.5 V using differential pulse voltammetry in a solution of 2.5 mM $Fe(CN)_6^{4-}$ and 0.1× PBS. Oxidation currents were measured before and after applying 30 μs and 10 ms 20 V pulses to the lysis electrodes at 1 Hz for 60 s.

To measure the amount of hybridized nucleic acid, electrochemical signals were measured in 0.1× PBS with 10 μM $[Ru(NH_3)_6]Cl_3$ and 4 mM $K_3[Fe(CN)_6]$. DPV signals were obtained with a potential step of 5 mV, pulse amplitude of 50 mV, pulse width of 50 ms, and a pulse period of 100 ms. Signal changes that corresponded to target hybridization were calculated with background-subtracted currents: $\Delta I = (I_{after} - I_{before})$ (where I_{after} = current after target hybridization and I_{before} = current before target hybridization, *i.e.*, current with only probe).

Conflict of Interest: The authors declare no competing financial interest.

Acknowledgment. This work was funded by CMC Microsystems, Ontario Research Fund, the Canadian Institute for Health Research, and the Natural Sciences and Engineering Research Council of Canada. We would like to extend our appreciation to Brian Lam for his advice throughout the project. We thank the ECTI facility at University of Toronto for their cleanroom facilities. We wish to acknowledge CMC Microsystems for their help with CAD design and fabrication services.

Supporting Information Available: Additional information on the diffusional model and supporting experiments are included as Supporting Information. This material is available free of charge *via* the Internet at http://pubs.acs.org.

REFERENCES AND NOTES

1. Mancini, N.; Carletti, S.; Ghidoli, N.; Cichero, P.; Burioni, R.; Clementi, M. The Era of Molecular and Other Non-culture-Based Methods in Diagnosis of Sepsis. *Clin. Microbiol. Rev.* **2010**, *23*, 235–251.
2. Ecker, D. J.; Sampath, R.; Li, H.; Massire, C.; Matthews, H. E.; Toleno, D.; Hall, T. A.; Blyn, L. B.; Eshoo, M. W.; Ranken, R.; *et al.* New Technology for Rapid Molecular Diagnosis of Bloodstream Infections. *Expert Rev. Mol. Diag.* **2010**, *10*, 399–415.
3. Bloos, F.; Hinder, F.; Becker, K.; Sachse, S.; Mekontso Dessap, A.; Straube, E.; Cattoir, V.; Brun-Buisson, C.; Reinhart, K.; Peters, G.; *et al.* A Multicenter Trial To Compare Blood Culture with Polymerase Chain Reaction in Severe Human Sepsis. *Intens. Care. Med.* **2010**, *36*, 241–247.
4. Ferguson, B. S.; Buchsbaum, S. F.; Wu, T.-T.; Hsieh, K.; Xiao, Y.; Sun, R.; Soh, H. T. Genetic Analysis of H1N1 Influenza Virus from Throat Swab Samples in a Microfluidic System for Point-of-Care Diagnostics. *J. Am. Chem. Soc.* **2011**, *133*, 9129–9135.
5. Lee, H.; Yoon, T.-J.; Weissleder, R. Ultrasensitive Detection of Bacteria Using Core−Shell Nanoparticles and an NMR-Filter System. *Angew. Chem., Int. Ed.* **2009**, *48*, 5657–5660.
6. Anker, J. N.; Hall, W. P.; Nilam, C.; Zhao, J.; Van, P. Biosensing with Plasmonic Nanosensors. *Nat. Mater.* **2008**, *7*, 8–10.
7. Chung, H. J.; Castro, C. M.; Im, H.; Lee, H.; Weissleder, R. A Magneto-DNA Nanoparticle System for Rapid Detection and Phenotyping of Bacteria. *Nat. Nanotechnol.* **2013**, *8*, 369–375.
8. Cederquist, K. B.; Kelley, S. O. Nanostructured Biomolecular Detectors: Pushing Performance at the Nanoscale. *Biotechnol. Adv.* **2012**, *16*, 415–421.
9. Foudeh, A. M.; Fatanat Didar, T.; Veres, T.; Tabrizian, M. Microfluidic Designs and Techniques Using Lab-on-a-Chip Devices for Pathogen Detection for Point-of-Care Diagnostics. *Lab Chip* **2012**, *12*, 3249–3266.
10. Lam, B.; Das, J.; Holmes, R. D.; Live, L.; Sage, A.; Sargent, E. H.; Kelley, S. O. Solution-Based Circuits Enable Rapid and Multiplexed Pathogen Detection. *Nat. Commun.* **2013**, *4*, 1–8.
11. Drummond, T. G.; Hill, M. G.; Barton, J. K. Electrochemical DNA Sensors. *Nat. Biotechnol.* **2003**, *21*, 1192–1199.
12. Sorgenfrei, S.; Chiu, C.; Gonzalez, R. L.; Yu, Y.-J.; Kim, P.; Nuckolls, C.; Shepard, K. L. Label-Free Single-Molecule Detection of DNA-Hybridization Kinetics with a Carbon Nanotube Field-Effect Transistor. *Nat. Nanotechnol.* **2011**, *6*, 126–132.

13. Hsieh, K.; Patterson, A. S.; Ferguson, B. S.; Plaxco, K. W.; Soh, H. T. Rapid, Sensitive, and Quantitative Detection of Pathogenic DNA at the Point of Care through Microfluidic Electrochemical Quantitative Loop-Mediated Isothermal Amplification. *Angew. Chem., Int. Ed.* **2012**, *51*, 4896–4900.
14. Zhang, J.; Song, S.; Zhang, L.; Wang, L.; Wu, H.; Pan, D.; Fan, C. Sequence-Specific Detection of Femtomolar DNA *via* a Chronocoulometric DNA Sensor (CDS): Effects of Nanoparticle-Mediated Amplification and Nanoscale Control of DNA Assembly at Electrodes. *J. Am. Chem. Soc.* **2006**, *128*, 8575–8580.
15. Adékambi, T.; Drancourt, M.; Raoult, D. The rpoB Gene as a Tool for Clinical Microbiologists. *Trends Microbiol.* **2009**, *17*, 37–45.
16. Sheehan, P. E.; Whitman, L. J. Detection Limits for Nanoscale Biosensors. *Nano Lett.* **2005**, *5*, 803–807.
17. Soleymani, L.; Fang, Z.; Lam, B.; Bin, X.; Vasilyeva, E.; Ross, A.; Sargent, E. H.; Kelley, S. O. Hierarchical Nanotextured Microelectrodes Overcome the Molecular Transport Barrier To Achieve Rapid, Direct Bacterial Detection. *ACS Nano* **2011**, *5*, 3360–3366.
18. Lam, B.; Fang, Z.; Sargent, E. H.; Kelley, S. O. Polymerase Chain Reaction-Free, Sample-to-Answer Bacterial Detection in 30 Minutes with Integrated Cell Lysis. *Anal. Chem.* **2011**, *84*, 21–25.
19. Smith, D. E.; Perkins, T. T.; Chu, S. Dynamical Scaling of DNA Diffusion Coefficients. *Macromolecules* **1996**, *29*, 1372–1373.
20. Lee, H. J.; Kim, J.-H.; Lim, H. K.; Cho, E. C.; Huh, N.; Ko, C.; Park, J. C.; Choi, J.-W.; Lee, S. S. Electrochemical Cell Lysis Device for DNA Extraction. *Lab Chip* **2010**, *10*, 626–633.
21. Jha, S. K.; Chand, R.; Han, D.; Jang, Y.-C.; Ra, G.-S.; Kim, J. S.; Nahm, B.-H.; Kim, Y.-S. An Integrated PCR Microfluidic Chip Incorporating Aseptic Electrochemical Cell Lysis and Capillary Electrophoresis Amperometric DNA Detection for Rapid and Quantitative Genetic Analysis. *Lab Chip* **2012**, *12*, 4455–4464.
22. Nevill, J. T.; Cooper, R.; Dueck, M.; Breslauer, D. N.; Lee, L. P. Integrated Microfluidic Cell Culture and Lysis on a Chip. *Lab Chip* **2007**, *7*, 1689–1695.
23. Lapierre, M. A.; O'Keefe, M.; Taft, B. J.; Kelley, S. O. Electrocatalytic Detection of Pathogenic DNA Sequences and Antibiotic Resistance Markers. *Anal. Chem.* **2003**, *75*, 6327–6333.
24. Lam, B.; Holmes, R. D.; Das, J.; Poudineh, M.; Sage, A.; Sargent, E. H.; Kelley, S. O. Optimized Templates for Bottom-Up Growth of High-Performance Integrated Biomolecular Detectors. *Lab Chip* **2013**, *13*, 2569–2575.
25. Bhatt, N.; Huang, P.-J. J.; Dave, N.; Liu, J. Dissociation and Degradation of Thiol-Modified DNA on Gold Nanoparticles in Aqueous and Organic Solvents. *Langmuir* **2011**, *27*, 6132–6137.